

The effect of deuteration on the optical spectra of compressed methane

Cite as: AIP Advances 9, 045033 (2019); <https://doi.org/10.1063/1.5095851>

Submitted: 13 March 2019 . Accepted: 17 April 2019 . Published Online: 29 April 2019

Ciprian G. Pruteanu 



View Online



Export Citation



CrossMark

ARTICLES YOU MAY BE INTERESTED IN

[Friction and wear properties of base oil enhanced by different forms of reduced graphene](#)

AIP Advances 9, 045011 (2019); <https://doi.org/10.1063/1.5089107>

AVS Quantum Science

Co-published with AIP Publishing



Coming Soon!

The effect of deuteration on the optical spectra of compressed methane

Cite as: AIP Advances 9, 045033 (2019); doi: 10.1063/1.5095851

Submitted: 13 March 2019 • Accepted: 17 April 2019 •

Published Online: 29 April 2019



View Online



Export Citation



CrossMark

Ciprian G. Pruteanu^{a)} 

AFFILIATIONS

Department of Physics and Astronomy, University College London, Gower Street, London WC1E 6B, United Kingdom

^{a)}Electronic mail: cip.pruteanu@ucl.ac.uk

ABSTRACT

The *in situ* high pressure Raman spectrum of CD₄ was found to be subtly different from its' hydrogenous analog, CH₄. High quality data were obtained for the first time for pressures between 12 and 20 GPa during both fast and slow compression. Similarly to CH₄ in phase B, CD₄ does exhibit peak splitting in the ν_1 (symmetric stretch) and ν_3 (antisymmetric stretch) modes, but having the emergent shoulders present on the high-frequency side of the peaks rather than the low-frequency one as in the case of CH₄. The general aspect of the Raman spectrum was found to be very different from that of CH₄, with modes ν_1 and ν_3 having comparable intensities and the latter being sharper and better defined, in stark contrast to how it appears in CH₄.

© 2019 Author(s). All article content, except where otherwise noted, is licensed under a Creative Commons Attribution (CC BY) license (<http://creativecommons.org/licenses/by/4.0/>). <https://doi.org/10.1063/1.5095851>

I. INTRODUCTION

Methane is the simplest hydrocarbon, of great importance from both a fundamental scientific and technological point of view. It is widespread in the Solar System¹ and a major constituent of the “Icy planets” and their moons such as Neptune, Uranus and Titan.^{2–4} This renders the behavior of high pressure methane crucial for both understanding the conditions and state of the aforementioned planets and for the development of robust computational models to be used in materials research. Being such a simple molecule, it is a model system upon which most computational forcefields widely used in biological sciences are built.⁵ Adding to its importance is also that it is one of the two components of natural gas hydrates, chemical compounds crucial for energy storage and production^{6,7} and an exceptionally potent greenhouse gas.⁸ Furthermore, high pressure has a very strong effect on the interaction between water and methane, causing a very large increase in the solubility of the later.⁹ Finally, Raman spectroscopy is one of the most powerful techniques in high pressure physics, being used to detect and characterize phases and phase transitions. This requires a very clear understanding of the impact of isotopic effects on the Raman signature of a material, allowing one to distinguish phases and transitions only present in deuterated samples and not in hydrogenous ones.¹⁰

There has been significant debate on the high pressure phases of methane at room temperature, owing at least partially to the high

content of hydrogen rendering a full structural solution by X-Ray Diffraction (XRD) prohibitively difficult. The early Raman studies performed by Hebert *et al.*¹¹ identified 3 solid phases for methane on compression to 20 GPa at room temperature. Phase I appears on crystallization from liquid at 1.6 GPa and was determined by Hazen *et al.*¹² to be a face-centered cubic structure (space group *Fm3m*) based on the carbon positions obtained from XRD. Around 5.2 GPa methane transforms to phase A, found by Maynard *et al.*¹³ to display a distorted close-packed, rhombohedral structure (space group *R3*). Upon further compression between 8 and 18 GPa another transition, deemed “sluggish”, to phase B occurs according to Bini *et al.*¹⁴ and independently confirmed by Hirai *et al.*¹⁵ The reason for calling the transition sluggish is that it occurs starting at 8 GPa but requires 16h of resting at said pressure for the sample to fully change. For a significant time, the existence of this phase has been disputed, with various studies claiming its absence or failure to detect it in the suggested pressure range.¹⁶ A full structural solution for this phase has not been presented yet, due to the known tendency of methane to form large-grained or textured powders. However, the carbon sublattice has been solved by Maynard *et al.*¹⁷ from XRD and revealed a crystal structure similar to α -Mn at ambient conditions (space group *I43m*), vastly different from the cubic close-packed structure widely-assumed by the community until then. Optically, the A \rightarrow B transition is easily distinguishable in hydrogenous methane, being characterized by very pronounced peak splitting in the ν_1 and ν_3

modes as shown by Chen *et al.*¹⁸ At higher pressures, the experimental evidence is split between some who claim to observe a further phase transition around 25 GPa^{15,19} and those who report no distinguishable changes, at least as far as the Raman spectra are concerned,¹⁸ but support such a possible transition at even higher pressures (around 40 GPa) to a phase named HP/HP1.

Part of the problem boils down to the A to B transition occurring slowly over several hours, which means that studies starting with the sample in phase A or below can entirely by-pass this particular transition by using an accelerated rate of compression, giving a direct A to HP/HP1 transition. To complicate issues further, in order to obtain a full structural solution, one needs to perform neutron scattering (in order to locate the hydrogen/deuterium atoms). This approach obviously relies on the assumption that any isotopic effect is small or negligible, which from the Raman studies of Wu *et al.*¹⁶ seemed to be the case, with the only effect of deuteration being a slight depression of the transition pressures (by 0.1-0.2 GPa). However, a study by Tao *et al.*²⁰ has revealed that deuteration can lift vibrational mode coupling hence breaking Fermi resonance,²¹ and so preferentially eliminates certain spectral features, posing concerns for direct comparisons between H/D analogues. These effects can be attributed to the different zero-point vibrational energies in deuterated and hydrogenous molecules. Additionally, more recent neutron diffraction studies²² performed on deuterated methane at low temperature have depicted a very different situation than what was believed based on Raman studies of hydrogenous methane. The authors noted no structural phase transitions at 25K in the 1-5 GPa range, being able to fit all the collected patterns with the rhombohedral structure corresponding to ambient temperature phase A. This leads naturally to asking the question: does methane display an isotope effect leading to entirely different phase diagrams for CH₄ and CD₄ (similar to larger molecules,²³ suggesting this effect is a fundamental one arising even in the smallest and simplest systems)? Alternatively, is the Raman signal so different for deuterated and hydrogenous samples that a direct phase-to-phase correspondence cannot be established?

This paper presents a study on CD₄ up to 20 GPa using *in situ* Raman spectroscopy inside Diamond Anvil Cells (DACs). This work extends significantly the pressure range over which the behavior of CD₄ has been investigated at room temperature, the only similar study being up to ~13 GPa by Wu *et al.*,¹⁶ which did not see the A to B transition in either hydrogenous or deuterated methane. In contrast to previous work, the present study benefits greatly from the use of modern, high quality, high signal-to-noise ratio Raman setups, avoiding misidentification of sample features due to noise or random fluctuations in the background.

II. EXPERIMENTAL METHOD

The samples were loaded in Merrill-Bassett (MB) diamond anvil cells²⁴ equipped with Bohler-Almax seats.²⁵ A ruby pellet (5 μm diameter sphere) was attached to a side of a drilled steel gasket hole (50 μm depth, 175 μm diameter) to allow for pressure determination via the ruby fluorescence method.^{26,27} A cylinder of CD₄ gas (Sigma-Aldrich Methane-d4 99%, CAS Number 558-20-3) was attached to a sealed and liquid nitrogen-cooled pot in which the open DAC has been placed. The pot was filled with methane as it was liquefying and once the cell was fully immersed in fluid CD₄ it

was closed and sealed. No pressure transmitting medium was necessary due to methane being highly compressible and able to maintain a hydrostatic pressure environment on its own. A 514.15 nm Ar emission laser (60 mW) along with an Acton SpectraPro spectrograph and Andor CCD camera (operating at -77°C) were used for the Raman measurements.

III. RESULTS AND DISCUSSION

A. Normal modes

To investigate the effect of equilibration time on the Raman spectrum observed from a sample (and determine whether the “sluggish” A \rightarrow B transition occurs in deuterated methane), the two cells were allowed to rest at different pressures for several days. The first sample (labeled “1st MB”) was left at 7 GPa (Fig. 1) while the second sample (labeled “2nd MB”) was allowed to rest at 12 GPa. It is worth mentioning that both samples when at 6 GPa yielded Raman spectra consistent with the ones previously reported by Wu and coworkers.

The present study focuses on the strongest visible peaks (Raman active modes) for CD₄, which are the $\nu_2(E)$ (the bending mode, around 1100 cm^{-1}), $\nu_1(A_1)$ (the symmetric stretch, ~2200 cm^{-1}) and the $\nu_3(F_2)$ (the antisymmetric stretch, around 2350 cm^{-1}).²⁸

The ν_2 mode showed a steady increase with pressure at a rate of ~4.2 $\text{cm}^{-1}/\text{GPa}$, in the 12-20 GPa region (Fig. 2). Despite the relatively low intensity of the Raman peak (in comparison to the ν_1 and ν_3 modes), it was possible to accurately determine its position and broadness. Further analysis after background subtraction and log intensity scaling did not reveal any fine structure and hence no peak splitting, as it is expected from fundamental molecular theory.

It is worth noticing the “over-shoot” (jump of the vibron frequency to a significantly higher wavenumber) of the sample that was allowed to rest at 7 GPa. This sample was suddenly compressed to 12.5 GPa prior to the measurement, and slightly later to 13.7 GPa. Both these measurements yielded a noticeably higher Raman frequency than the equivalent ones performed on the cell that was

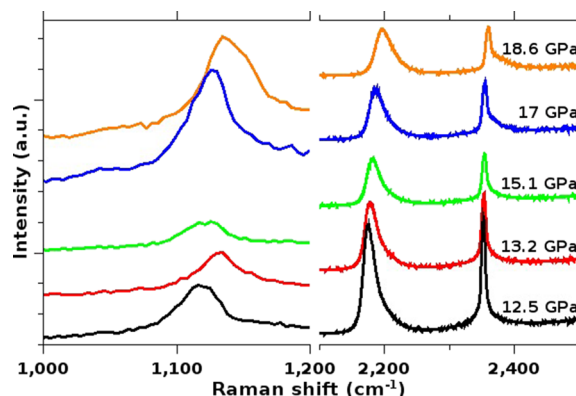


FIG. 1. Unprocessed Raman spectra of vibrational modes of CD₄ of a sample rested at 7 GPa for several days prior to sudden compression to 12.5 GPa (labeled “1st MB” throughout the text).

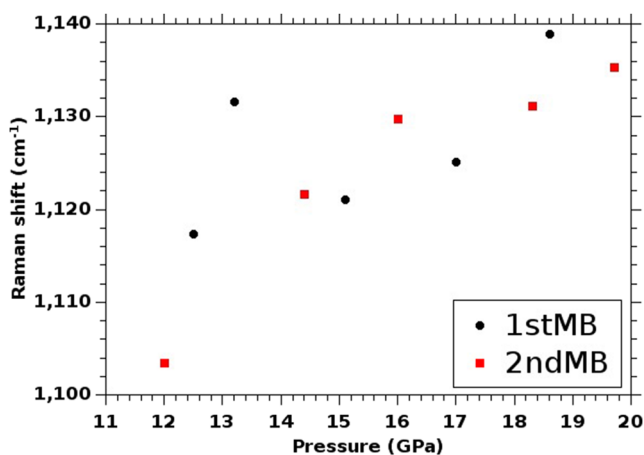


FIG. 2. Evolution of the ν_2 mode with pressure. A clear difference in the evolution of the mode's frequency with pressure between the rested sample ("2nd MB") and the one undergoing fast compression prior to the measurement ("1st MB").

allowed to rest at 12 GPa prior to the experimental run. This situation suggests a relatively strong dependence of the ν_2 mode on the recent history of the sample, allowing this mode to be used to assess whether the sample reached equilibrium or not.

In stark contrast to ν_2 , the ν_1 mode does not show any noticeable sudden jumps in its frequency depending on the recent history of the sample (Fig. 3). Throughout the entire pressure range considered in this study, the peak appeared broad and asymmetric, displaying an identifiable shoulder on the high-frequency side. The difference between the main peak and this shoulder was determined to be $\sim 25 \text{ cm}^{-1}$ and seemed independent of pressure. The magnitude of the splitting is consistent with previous measurements on hydrogenous methane at similar pressures,¹⁸ taking into account that the magnitude of peak splitting in degenerate modes is inversely proportional to the mass of the atoms involved in bonding, and since the mass of deuterium is almost twice the mass of hydrogen the

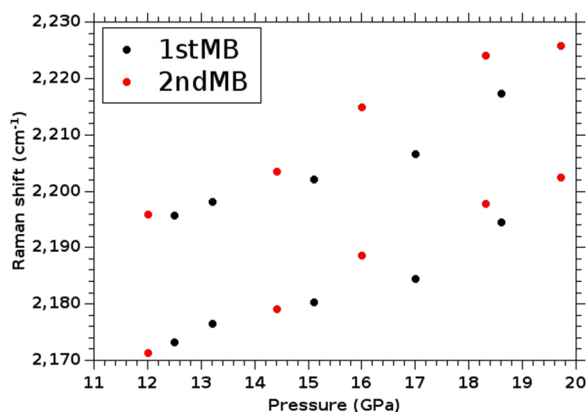


FIG. 3. Evolution of the ν_1 mode with pressure. The peak was asymmetric through the entire compression range, exhibiting an identifiable shoulder on the high-frequency side.

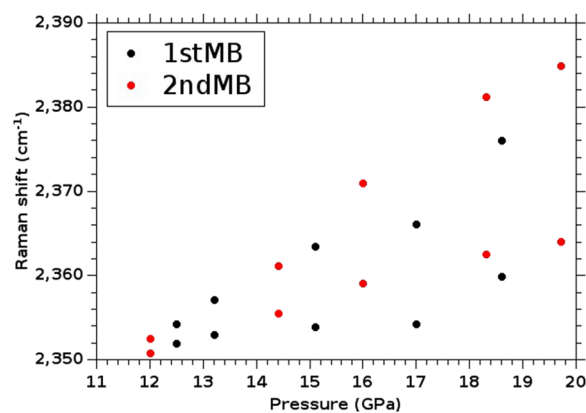


FIG. 4. Evolution of the ν_3 mode with pressure. The Raman peak displayed a clear high-frequency shoulder through the entire compression range that became better defined with increasing pressure.

splitting is significantly reduced. Overall, in the 12–20 GPa region the ν_1 mode shows an increase of $3.8 \text{ cm}^{-1}/\text{GPa}$, significantly lower than the $\sim 6.3 \text{ cm}^{-1}/\text{GPa}$ increase displayed at lower pressures.¹⁶

Lastly, the ν_3 mode's behavior resembles the one of the symmetric stretch mode at least to some extent (Fig. 4). There is a noticeable high-frequency shoulder at all pressures which becomes better defined with increasing pressure. However, in contrast to the ν_1 vibron, the magnitude of the splitting seems strongly pressure-dependant, growing linearly from $\sim 2 \text{ cm}^{-1}$ at 12 GPa to $\sim 20 \text{ cm}^{-1}$ at 19.7 GPa. This leads the lower-frequency component to shift at a rate of $\sim 1.5 \text{ cm}^{-1}/\text{GPa}$ and the higher frequency shoulder at $\sim 3.5 \text{ cm}^{-1}/\text{GPa}$.

In stark contrast to hydrogenous methane, in CD_4 the shoulders for ν_1 and ν_3 appeared on the high-frequency side of the main modes. Furthermore, all the measurements performed on the sample undergoing rapid $7 \rightarrow 12.5$ GPa compression prior to the measurement yielded noticeably lower frequencies throughout the entire pressure range that the sample allowed to rest at 12 GPa for several days. This mirrors the situation reported in CH_4 by Bini *et al.*,¹⁴ where after undergoing the $A \rightarrow B$ transition the Raman peaks positions shift to higher wavenumber over time until equilibrium is reached, supporting a phase transition in CD_4 below 12 GPa.

B. Full width at half maximum

In contrast to hydrogenous methane, where the ν_3 mode is very weak and broad, the current study found this peak to be exceptionally sharp and well-defined. The mode displayed a full-width at half maximum (FWHM) of $\sim 7 \text{ cm}^{-1}$ that seemed largely independent of pressure changes. This is a notable effect of deuteration, suggesting a stark difference between CD_4 and CH_4 in their internal vibrational behavior.

As seen in Fig. 5, while the ν_1 and ν_3 modes show little to no sensitivity to the previous state of the sample (quick compression vs. equilibrated at 12 GPa for days), the ν_2 mode seems more affected. Throughout the entire run, the measured ν_2 peak from the sample that underwent the rapid $7 \rightarrow 12$ GPa change remained sharper than

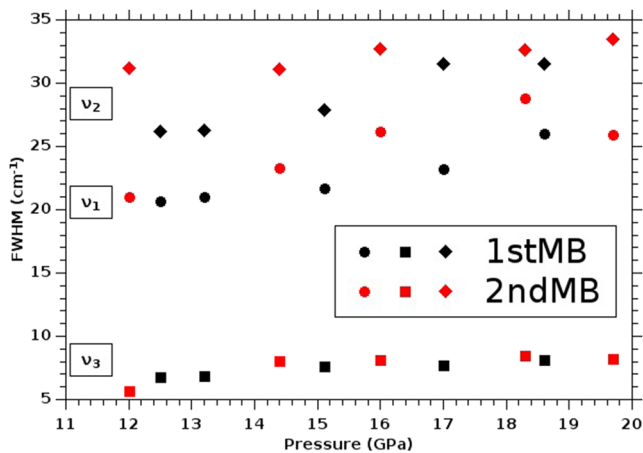


FIG. 5. Full width at half maximum for the ν_1 , ν_2 and ν_3 modes of CD_4 . The widths increase smoothly with pressure, not showing any indication of a phase transition.

the same peak measured from the sample rested at 12 GPa for a prolonged time. The gap in FWHM is narrowing as pressure is further increased, converging at a pressure of ~ 18 GPa.

Equally relevant is that the sample which started the experimental run at 12 GPa after resting at this pressure for several days displayed minimal broadening of the ν_2 peak as a function of pressure. This suggests that in a CD_4 sample properly equilibrated at a certain pressure (and probably in a certain phase) the sharpness of the ν_2 peak is largely independent of further pressure increase.

In what concerns the shoulders of the ν_1 (denoted ν_1') and ν_3 (denoted ν_3') modes, there seems to be little overall effect of increasing pressure on their broadness (Fig. 6). The analysis is further complicated in the case of ν_1' by the fact that it remains at the same separation from ν_1 at all pressures, making their clear identification problematic. In the case of ν_3' the identification is aided by the fact that the peak has almost double the pressure-induced shift

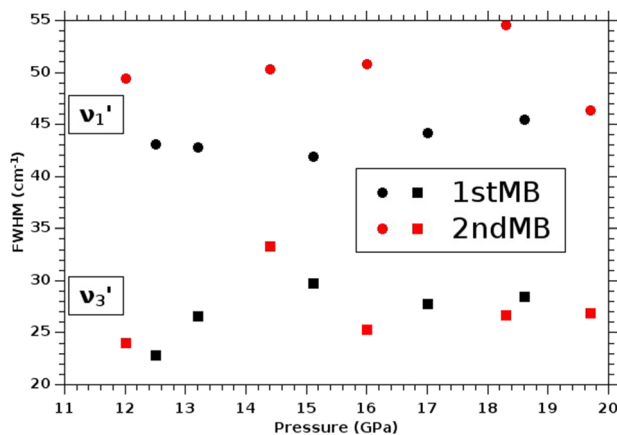


FIG. 6. Full width at half maximum for the ν_1' and ν_3' modes of CD_4 . These widths correspond to the higher-frequency components of the ν_1 and ν_3 modes as obtained from Gaussian decomposition.

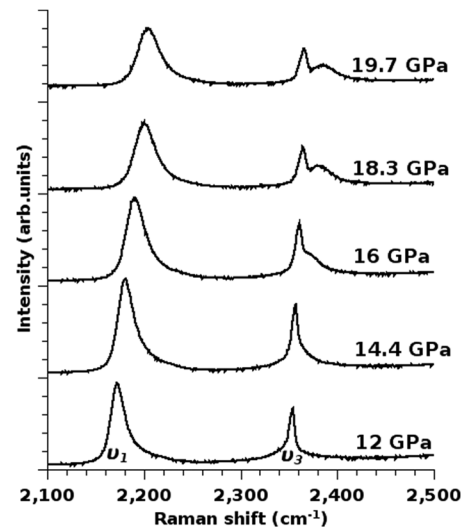


FIG. 7. ν_1 and ν_3 vibrons of CD_4 as a function of pressure for “2nd MB”. Around 16 GPa there is a clear emergence of a shoulder on the high-frequency side of ν_3 . All spectra are shown as recorded.

of ν_3 as mentioned beforehand, hence being almost fully separated at 19.7 GPa in sample “2nd MB” (Fig. 7).

C. The A to B phase transition

The data presented thus far paints a subtly different image for CD_4 than for CH_4 . Both the ν_1 and ν_3 vibrons show strong signs of splitting throughout the entire pressure range studied which covers the phase space corresponding to phase B in CH_4 . However, while in hydrogenous methane the shoulders appear on the low-frequency side of the main peak, in all of the current measurements these appeared on the high-frequency side. The rates of change in the ν_1 , ν_2 and ν_3 peak positions with pressure are extremely different from the ones previously reported at lower pressures. The current study found these to be $3.8 \text{ cm}^{-1}/\text{GPa}$ for ν_1 , $4.2 \text{ cm}^{-1}/\text{GPa}$ for ν_2 and only $1.5 \text{ cm}^{-1}/\text{GPa}$ for the main component of ν_3 in the 12–20 GPa range. This is in strong opposition to the situation at lower pressure, where the values for the rates would be 6.3 , 1.3 and $7.2 \text{ cm}^{-1}/\text{GPa}$ respectively.¹⁶ A similar behavior was also determined for the shoulders ν_1' and ν_3' , with the current study finding rates of $\sim 3.8 \text{ cm}^{-1}/\text{GPa}$ and $3.5 \text{ cm}^{-1}/\text{GPa}$ respectively, in contrast to 4.7 and $7.3 \text{ cm}^{-1}/\text{GPa}$ at lower pressures.

The different rates are consistent with the additional observation that at lower pressures all the shoulders were identified on the low-frequency side of the main peak, while the current study found them on the higher side. In addition to this, while at lower pressures the ν_3' peak is weak and hardly detectable, it becomes progressively better defined with increasing pressure, to the point of being almost fully separated from ν_3 by 19 GPa.

From the data and analysis presented thus far the author is led to conclude that the crystal phase observed in the present study is most likely phase B. The clear lifting of the degeneracy of the ν_3 mode coupled with its relative intensity in comparison to ν_1 which is at all points broad and asymmetric, along with the very different

rates of peak shift with pressure suggest the phase observed in the current study is different from the one reported by Wu *et al.*¹⁶

In addition to this, as noted throughout the paper there is a clear general trend of the sample that underwent rapid compression (7 → 12.5 GPa, labelled “1st MB”) to ‘lag’ behind the sample that was allowed to rest at 12 GPa prior to the measurement (“2nd MB”). This delay is visible both in the Raman peak positions and in the full width at half maximum to a certain extent (obvious in the case of the ν_2 mode). This is a well-known signature of “sluggish” phase transitions, further supporting the conclusion drawn in the previous paragraph.

IV. CONCLUSIONS

The behavior of CD₄ was investigated at pressures up to 19.7 GPa using Raman spectroscopy. The present study found that in the 12 → 19 GPa range CD₄ displays a Raman spectrum commensurate with that of phase B of hydrogenous methane but with some notable differences. The main distinctive feature of phase B in CH₄ is the strong splitting of the ν_1 and ν_3 bands, with clear shoulders appearing on their low-frequency sides. In CD₄ the shoulders are also present, but on the high-frequency side of the main vibrons. This suggests deuteration has a strong impact upon the Raman signal, possibly due to zero point energy effects that significantly alter the features of CH₄. Moreover, while in CH₄ the ν_3 mode is rather broad and weak in comparison to ν_1 , in CD₄ they have a comparable intensity, and ν_3 is the sharper and better defined of the two. Similarly to its hydrogenous analog, CD₄ was found to display a very strong time dependence when undergoing rapid compression to phase B. This has subtle but crucial implications for the detectable Raman spectrum, and such changes are likely to be overlooked if compression is performed over a short amount of time without allowing the sample to rest after each pressure increment. All these considerations highlight the difficulty of correlating crystal phases between deuterated and hydrogenous analogs of the same molecule by Raman spectroscopy.

ACKNOWLEDGMENTS

The author would like to thank Dr. Robin Turnbull for assistance when performing the Raman measurements, Drs. John Loveday, Andrew Seel, Chris Howard, Profs. Christoph Salzmann and Neal Skipper for a critical reading of the manuscript.

REFERENCES

- ¹K. Lodders, “Solar system abundances and condensation temperatures of the elements,” *The Astrophysical Journal* **591**, 1220 (2003).
- ²C. De Bergh, B. Lutz, T. Owen, J. Brault, and J. Chauville, “Monodeuterated methane in the outer solar system. II-Its detection on uranus at 1.6 microns,” *The Astrophysical Journal* **311**, 501–510 (1986).
- ³C. De Bergh, B. Lutz, T. Owen, and J. Chauville, “Monodeuterated methane in the outer solar system. III-Its abundance of titan,” *The Astrophysical Journal* **329**, 951–955 (1988).
- ⁴C. De Bergh, B. Lutz, T. Owen, and J.-P. Maillard, “Monodeuterated methane in the outer solar system. IV-Its detection and abundance on neptune,” *The Astrophysical Journal* **355**, 661–666 (1990).
- ⁵A. L. Rabinovich, P. O. Ripatti, and N. K. Balabaev, “Molecular dynamics investigation of bond ordering of unsaturated lipids in monolayers,” *Journal of Biological Physics* **25**, 245–262 (1999).
- ⁶K. A. Kvenvolden, “Gas hydrates-geological perspective and global change,” *Reviews of Geophysics* **31**, 173–187, <https://doi.org/10.1029/93rg00268> (1993).
- ⁷E. D. Sloan, Jr., “Fundamental principles and applications of natural gas hydrates,” *Nature* **426**, 353 (2003).
- ⁸D. Feldman, W. Collins, S. Biraud, M. Risser, D. Turner, P. Gero, J. Tadić, D. Helmig, S. Xie, E. Mlawer *et al.*, “Observationally derived rise in methane surface forcing mediated by water vapour trends,” *Nature Geoscience* **11**, 238 (2018).
- ⁹C. G. Pruteanu, G. J. Ackland, W. C. Poon, and J. S. Loveday, “When immiscible becomes miscible-methane in water at high pressures,” *Science Advances* **3**, e1700240 (2017).
- ¹⁰X.-D. Liu, R. T. Howie, H.-C. Zhang, X.-J. Chen, and E. Gregoryanz, “High-pressure behavior of hydrogen and deuterium at low temperatures,” *Physical Review Letters* **119**, 065301 (2017).
- ¹¹P. Hebert, A. Polian, P. Loubeyre, and R. Le Toullec, “Optical studies of methane under high pressure,” *Physical Review B* **36**, 9196 (1987).
- ¹²R. Hazen, H. Mao, L. Finger, and P. Bell, “Structure and compression of crystalline methane at high pressure and room temperature,” *Applied Physics Letters* **37**, 288–289 (1980).
- ¹³H. Maynard-Casely, C. Bull, M. Guthrie, I. Loa, M. McMahon, E. Gregoryanz, R. Nelmes, and J. Loveday, “The distorted close-packed crystal structure of methane a,” *The Journal of Chemical Physics* **133**, 064504 (2010).
- ¹⁴R. Bini, L. Ulivi, H. J. Jodl, and P. R. Salvi, “High pressure crystal phases of solid CH₄ probed by fourier transform infrared spectroscopy,” *The Journal of Chemical Physics* **103**, 1353–1360 (1995).
- ¹⁵H. Hirai, K. Konagai, T. Kawamura, Y. Yamamoto, and T. Yagi, “Phase changes of solid methane under high pressure up to 86 GPa at room temperature,” *Chemical Physics Letters* **454**, 212–217 (2008).
- ¹⁶Y. Wu, S. Sasaki, and H. Shimizu, “High-pressure Raman study of dense methane: CH₄ and CD₄,” *Journal of Raman Spectroscopy* **26**, 963–967 (1995).
- ¹⁷H. Maynard-Casely, L. Lundegaard, I. Loa, M. McMahon, E. Gregoryanz, R. Nelmes, and J. Loveday, “The crystal structure of methane B at 8 GPa-An α -Mn arrangement of molecules,” *The Journal of Chemical Physics* **141**, 234313 (2014).
- ¹⁸P.-N. Chen, C.-S. Zha, X.-J. Chen, J. Shu, R. J. Hemley, and H.-k. Mao, “Raman study of phase transitions in compressed methane using moissanite anvil cells,” *Physical Review B* **84**, 104110 (2011).
- ¹⁹S. Umemoto, T. Yoshii, Y. Akahama, and H. Kawamura, “X-ray diffraction measurements for solid methane at high pressures,” *Journal of Physics: Condensed Matter* **14**, 10675 (2002).
- ²⁰Y. Tao, Z. A. Dreger, and Y. M. Gupta, “High-pressure stability of 1, 1-diamino-2, 2-dinitroethene (FOX-7): H/D isotope effect,” *Chemical Physics Letters* **624**, 59–63 (2015).
- ²¹L. Wiesenfeld, “The vibron model for methane: Stretch–Bend interactions,” *Journal of Molecular Spectroscopy* **184**, 277–287 (1997).
- ²²H. Maynard, J. Loveday, S. Klotz, C. Bull, and T. Hansen, “High-pressure crystallography of methane: A low-temperature neutron diffraction study in the 1–5 GPa range,” *High Pressure Research* **29**, 125–128 (2009).
- ²³T. Matsuo, A. Inaba, O. Yamamuro, and N. Onoda-Yamamuro, “Proton tunnelling and deuteration-induced phase transitions in hydrogen-bonded crystals,” *Journal of Physics: Condensed Matter* **12**, 8595 (2000).
- ²⁴L. Merrill and W. A. Bassett, “Miniature diamond anvil pressure cell for single crystal x-ray diffraction studies,” *Review of Scientific Instruments* **45**, 290–294 (1974).
- ²⁵R. Boehler, “New diamond cell for single-crystal x-ray diffraction,” *Review of Scientific Instruments* **77**, 115103 (2006).
- ²⁶G. J. Piermarini, S. Block, J. Barnett, and R. Forman, “Calibration of the pressure dependence of the R1 ruby fluorescence line to 195 kbar,” *Journal of Applied Physics* **46**, 2774–2780 (1975).
- ²⁷H. Mao, P. Bell, J. t. Shaner, and D. Steinberg, “Specific volume measurements of Cu, Mo, Pd, and Ag and calibration of the ruby R1 fluorescence pressure gauge from 0.06 to 1 Mbar,” *Journal of Applied Physics* **49**, 3276–3283 (1978).
- ²⁸G. Magnotti, U. KC, P. Varghese, and R. Barlow, “Raman spectra of methane, ethylene, ethane, dimethyl ether, formaldehyde and propane for combustion applications,” *Journal of Quantitative Spectroscopy and Radiative Transfer* **163**, 80–101 (2015).